Nutrient-dependent growth underpinned the Ediacaran transition to large body size

Jennifer F. Hoyal Cuthill[1,2*] and Simon Conway Morris[2]

[1]Earth-Life Science Institute, Tokyo Institute of Technology, Tokyo, 152-8550, Japan

[2]Department of Earth Sciences, University of Cambridge, CB2 3EQ, UK

Macro-scale rangeomorph fossils, with characteristic branching fronds, appear (571 Ma) after the Gaskiers glaciation (580 Ma). However, biological mechanisms of size growth, and potential connections to ocean geochemistry, were untested. Using micro-CT and photographic measurements, alongside mathematical and computer models, we demonstrate that growth of rangeomorph branch internodes declined as their relative surface area decreased. This suggests that frond size and shape were directly responsive to nutrient uptake.

Early representatives of the Ediacaran macro-biota include the rangeomorphs, characterised by an approximately fractal, branching morphology [1, 2]. Reaching up to 2 m in length [3], rangeomorphs from the Drook Formation, Newfoundland (571 Ma [4]) show a size increase of 1-2 orders of magnitude in comparison with most earlier organisms [5, 6] (though see also [7, 8]). Their large size and morphological differentiation (with a frond and holdfast) class rangeomorphs within the major evolutionary transition to complex multicellularity [5, 6, 9]. Furthermore, geological evidence for deep-marine habitats rules out photosynthesis but is compatible with heterotrophy [10]. Consequently, they are widely viewed as, at least, opisthokonts and, likely, early metazoans [11]. A key question, then, is why large rangeomorph fossils appeared suddenly [3], potentially 1 billion years after eukaryotes first evolved [8] but some 30 Ma before the Cambrian explosion of animal diversity.

Here we propose and test the hypothesis that rangeomorph growth was nutrient-dependent due to feedbacks between branch volume, relative surface area and nutrient

uptake. This provides a developmental mechanism to link the appearance of large body size with postulated regional increases in nutrients that limit aerobic heterotrophy (particularly oxygen and organic carbon [12]) [13].

Along the stem (zero-order branch [2]) of the rangeomorph *Avalofractus abaculus* (Fig. 1a), micro-CT size measurements (Tables S1-S3) indicate negative feedback between internode size and proportionate size growth (the proportion by which size increased at each growth step). Based on vertically retrodeformed stem diameter and measured stem length (Fig. 1b, Figs. S1, S3-S4), the calculated surface area to volume ratio (SA/V) of the stem evidently declined as its internodes (segments of the stem between sequential lateral branches, Fig. 1) increased in number, age and size (Fig. S5). Correspondingly, while the volumes of sequential internodes increase along the age series, the proportionate increase in volume between them fell at each growth step (Fig. 2a, Fig. S6, log10 transformed data linear regression slope = -0.42, intercept = -0.83, R^2 = 0.64, p = 0.0019). Thus, proportionate branch growth declined as volume increased relative to surface area. These results are closely matched by computer simulations using a simple model of nutrient-dependent growth in which volume growth is proportionate to the change in SA/V, although the precise simulation results depend on the specified growth parameter values (e.g. linear regression slope -0.37, with initial volume growth of 1000%, Fig. S7a). This is in marked contrast to the slope of zero predicted under a null model of unlimited exponential growth, where the proportion of volume added at each growth step remains constant. Crucially, therefore, proportionate size growth in *Avalofractus* was greater for younger branch segments which had a relatively large external surface to provision their internal volume. This suggests a positive dependence of growth on nutrient uptake across the surface of the branches (Fig. 3b).

We then compared the spacing of lateral branches in an apical-basal series (illustrated Fig. 1a), measured from digital photographs of two additional rangeomorph specimens (Table

S5), against 1D predictions for stem length (Figs. S9-S10) generated from the theoretical 3D growth models. In each case, a slower growing, quadratic curve, consistent with the nutrient-dependent growth model, was supported with > 99.9% probability over the null hypothesis of rapid, exponential growth (Fig. 2b-d). A quadratic curve is also the best fitting model, with > 99.7% probability, when compared against a linear regression (Fig. S12).

The measured decline in proportionate size growth between sequential stem internodes of the rangeomorph frond (Fig. 2) is consistent with growth strongly limited by uptake of nutrients into local tissue. Based on micro-CT measurements at the base of the stem of *Avalofractus abaculus*, the maximum calculated diameter was 1.2 mm, with radius 0.6 mm (Fig. 1). Due to the finely branched structure of the frond, most branches have diameters considerably below this basal maximum (with the width of the smallest preserved branches measured at <150 µm [1]). For this small individual, the maximum radius of 0.6 mm is within the maximum oxygen diffusion depth of 1 mm previously estimated for modern marine invertebrates [14]. Similarly, experiments on young sponge explants (which lacked a well-developed water canal system) show that diffusion of oxygen (at present atmospheric level, PAL) and DOC (<0.22 µm, >300 mg l^{-1}) through the body surface can sustain metabolically active tissue to a thickness of ~1 mm, above which explants may develop a necrotic core and die [15]. Mechanisms to circumvent limits on body exterior-to-interior nutrient diffusion, similar to those seen in living animals, may have been employed to survive at very low oxygen levels (e.g. < 4% PAL [16]) or to achieve larger stem diameters (e.g. in large rangeomorph individuals). These could include restriction of metabolically active cells to shallow tissue depths (< 1mm), via reduction in cell density, a metabolically inactive internal matrix (e.g. mesoglea) or hollow interior [11], incorporation of surface pores or canals, or active water pumping (e.g. with choanocytes) [17, 18].

Computer simulations of nutrient-dependent growth in internode size (using a generalisation of the alternate branching pattern common to the rangeomorphs [2]) demonstrate aggregate effects on the size and shape of the entire frond (Fig. 3). Compared to the null hypothesis of exponential growth (Fig. 3a), nutrient-dependent growth is also partitioned so that the greatest proportionate growth occurs in the smallest branches, which have the highest surface area to volume ratio (Fig. 3b, Table S4). This, in turn, generates a frond with a greater total surface area relative to both internal volume and bounding volume.

These results imply that nutrient-dependent growth formed a key component in the Ediacaran transition to large body size. This nutrient-dependent growth programme is automatically responsive to environmental nutrient levels (Fig. 3d-e, Table S4). Unsurprisingly, but intriguingly, such nutrient-growth interactions generate different morphologies under different environmental conditions. Higher nutrient levels enable a greater total body size to be achieved within the same number of branching growth steps (Fig. 3 d-e). Nutrient-dependent branch growth also affects frond shape. A vertically increasing nutrient gradient [19], for example, results in a relatively narrower frond, and a tapered frond shape due to reduced growth of the basal lateral branches (Fig. 3e). Since the underlying growth programme is identical (Fig. 3c-e), this morphological variation is ecophenotypic, with differences determined entirely by feedback between nutrient uptake, growth and size (Fig. 3b). Our results therefore support previous suggestions of ecophenotypic variation among Ediacaran macro-organisms [20] and provide an explicit developmental mechanism in the form of nutrient-dependent growth. Given apparently wide temporal and regional fluctuations in geochemistry throughout the late Proterozoic [13, 21, 22], this wide reaction norm may itself have been adaptive.

Methods

Avalofractus abaculus stem widths were measured at 0.33 mm length intervals on virtual transverse sections from a micro-CT volume rendering of cast ROM 63005 [11] (voxel size resolution 0.049 mm, CT data provided at the Dryad data repository, doi:10.5061/dryad.47n27). Widths were vertically retrodeformed to correct diameter for post-mortem compaction (Fig. S1). Surface area (Supplementary Methods, SM Eqn. 1) and volume (SM Eqn. 2) of sequential stem internodes (indicated Fig. 1), were calculated using apical and basal internode radii from a linear relationship between stem length and diameter (grey line, Fig. 1). This was the best-fit of four theoretical curves [23] representing isometric (linear) versus negative or positive allometric scaling of length to diameter (Fig. 1, Figs. S3-S4).

Growth in size of rangeomorph branch internodes was simulated (Supplementary Computer Code) with models of nutrient-dependent growth (SM Eqn. 9), a vertical nutrient gradient, and a null model of exponential volumetric growth (SM Eqn. 3).

Theoretical 3D volumetric growth models were used to generate 1D predictions for growth in length (Figs. S9-S10). This enabled model testing for stem length growth (Fig. 2, Fig. S11-12) additionally based on digital photographs of the holotype of *Charnia masoni* and an undescribed South Australian museum rangeomorph.

See Supplementary Methods for further details.

Data Availability

All measured data and computer code are provided in this published article and the Supplementary Information. Micro-CT data are available in the Dryad Digital Repository.

Figure Legends

Figure 1. Retrodeformed stem diameter b, measured from a 3D micro-CT volume rendering of *Avalofractus abaculus* cast ROM 63005, a. Arrows indicate origination points of 14 sequential lateral branches (right, blue; left, red). Stem regions between adjacent lateral branches are internodes in an ordinal age series (youngest, apical, left; oldest, basal, right). Grey dashed line indicates a theoretical isometric scaling relationship of diameter = length × 0.05 (R^2 = 0.37, Figs. S3-S4).

Figure 2. Sequential stem internode volumes (a) and lengths (b-d), from micro-CT (a-b) and digital photographs (c-d) of rangeomorph specimens. a-b, *Avalofractus abaculus* specimen ROM 63005 (Fig. 1a). **c**, *Charnia masoni* holotype (replica). **d**, Undescribed South Australian Museum specimen. Calculated volumes (**a**) of 13 sequential stem internodes of *Avalofractus abaculus* (shown, Fig.1). Linear regression (black line) slope = -0.42, intercept = -0.83, R^2 = 0.64, p = 0.0019. **b-d**, Fitted quadratic curves (blue lines), supporting nutrient-dependent growth (Fig. S10). Fitted null hypothesis (red lines) of exponential growth (Fig. S9). Akaike Information Criterion, *AICc*, (quadratic, exponential) and corresponding likelihood that the quadratic curve is a better model: **b**, -27.69, -13.96, 99.8957%; **c**, 53.24, 97.73, 100%; **d**, -26.38, 30.50, 100%. Bands: 95% confidence (darker) and 95% prediction (lighter). Reversed axes (Fig. S11a), proportionate data (Fig. S11b), linear regressions (Fig. S12).

Figure 3. Computer simulations of rangeomorph internode size growth. a, Exponential growth of branch internodes. **b,** Diagram illustrating feedback between nutrient uptake, growth and size. Arrows indicate positive (blue) versus negative (red) effects. **c-e**, Nutrient-dependent growth. **e**, Increasing nutrient gradient (darker background shading). Internode colours indicate the relative proportion of volume by which segments will grow at the next

step (blue, high; red, low). Growth steps: 3 (**a**,**c**) or 8 (**d**,**e**). Horizontal position (x axis) versus vertical position (y axis) in arbitrary units.

References

1. Narbonne, G. M., Modular construction of early Ediacaran complex life forms. *Science* **305**, 1141-1144 (2004).

2. Hoyal Cuthill, J. F. & Conway Morris, S., Fractal branching organizations of Ediacaran rangeomorph fronds reveal a lost Proterozoic body plan. *Proc. Natl. Acad. Sci. USA* **111** (36), 13122-13126 (2014).

3. Narbonne, G. M. & Gehling, J. G., Life after snowball: the oldest complex Ediacaran fossils. *Geology* **31**, 27-30 (2003).

4. Pu, J. P. *et al.*, Dodging snowballs: geochronology of the Gaskiers glaciation and the first appearance of the Ediacaran biota. *Geology* **44**, 955-958 (2016).

5. Butterfield, N. J., Modes of pre-Ediacaran multicellularity. *Precambrian Res.* **173**, 201-211 (2009).

6. Payne, J. L. *et al.*, Two-phase increase in the maximum size of life over 3.5 billion years reflects biological innovation and environmental opportunity. *Proc. Natl. Acad. Sci. USA* **106**, 24-27 (2009).

7. Yuan, X., Chen, Z., Xiao, C., Zhou, C. & Hua, H., An early Ediacaran assemblage of macroscopic and morphologically differentiated eukaryotes. *Nature* **470**, 390-393 (2011).

8. Zhu, S. *et al.*, Decimetre-scale multicellular eukaryotes from the 1.56-billion-year-old Gaoyuzhuang Formation in North China. *Nat. Commun.* **7**, DOI: 10.1038 (2016).

9. Szathmary, E. & Maynard Smith, J., The major evolutionary transitions. *Nature* **374**, 227-232 (1995).

10. Sperling, E. A., Peterson, K. J. & Laflamme, M., Rangeomorphs, *Thectardis* (Porifera?) and dissolved organic carbon in the Ediacaran oceans. *Geobiology* **9**, 24-33 (2011).

11. Narbonne, G. M., Laflamme, M., Greentree, C. & Trusler, P., Reconstructing a lost world: Ediacaran rangeomorphs from Spaniard's Bay, Newfoundland. *J. Paleont.* **83**, 503-523 (2009).

12. Laflamme, M., Xiao, S. & Kowalewski, M., Osmotrophy in modular Ediacara organisms. *Proc. Natl. Acad. Sci. USA* **106**, 14438-14443 (2009).

13. Canfield, D. E., Poulton, S. W. & Narbonne, G. M., Late-Neoproterozoic deep-ocean oxygenation and the rise of animal life. *Science* **315**, 92-95 (2007).

14. Runnegar, B., Oxygen requirements, biology and phylogenetic significance of the later Precambrian worm Dickinsonia, and the evolution of burrowing habit. *Alcheringa* **6**, 223-239 (1982).

15. Garcia Camacho, F. *et al.*, A bioreaction-diffusion model for growth of marine sponge explants in bioreactors. *Appl. Microbiol. Biotechnol.* **73**, 525-532 (2006).

16. Mills, D. B. *et al.*, Oxygen requirements of the earliest animals. *Proc. natl. Acad. Sci. USA* **111**, 4168-4172 (2014).

17. Budd, G. E. & Jensen, S., The origin of animals and a 'Savannah' hypothesis for early bilaterian evolution. *Biol. Rev.*, DOI: 10.1111/brv.12239 (2015).

18. Cavalier-Smith, T., Origin of animal multicellularity: precursors, causes, consequences-the choanoflagellate/sponge transition, neurogenesis and the Cambrian explosion. *Phil. Trans. R. Soc. B* **372**, 20151476 (2017).

19. Ghisalberti, M. *et al.*, Canopy flow analysis reveals the advantage of size in the oldest communities of multicellular eukaryotes. *Curr. Biol.* **24**, 1-5 (2014).

20. Brasier, M. D. & Antcliffe, J. B., Evolutionary relationships within the Avalonian Ediacara biota: new insights from laser analysis. *J. Geol. Soc. London* **166**, 363-384 (2009).

21. Sahoo, S. K. *et al.*, Ocean oxygenation in the wake of the Marinoan glaciation. *Nature* **489**, 546-549 (2012).

22. Sperling, E. A. *et al.*, Statistical anlaysis of iron geochemical data suggests limited late Proterozoic oxygenation. *Nature* **523**, 451-454 (2015).

23. Niklas, K. J., Size-dependent allometry of tree height, diameter and trunk-taper. *Ann. Bot.* **75**, 217-227 (1995).

Acknowledgements Specimen number ROM 63005 was loaned by the Royal Ontario Museum with the permission of the Rooms Museum, Newfoundland. CT-scanning was conducted by R. Asher at the Cambridge Biotomography Centre. Access to the specimen of Fig. 2d was provided at the South Australian Museum by J. Gehling and M.-A. Binnie, who found this fossil. This research was funded by an ELSI Origins Network (EON) Research

Fellowship to J.F.H.C., supported by a grant from the John Templeton Foundation, and Palaeontological Association Research Grant number PA-RG201501 (J.F.H.C). We thank N. Butterfield, A. Caulton and E. Smith for discussion of the manuscript.

Author Contributions

J.F.H.C designed and carried out the analysis; J.F.H.C. and S.C.M. co-wrote the paper.

Conflict of Interest Statement

The authors declare no conflict of interest.

Figure 1

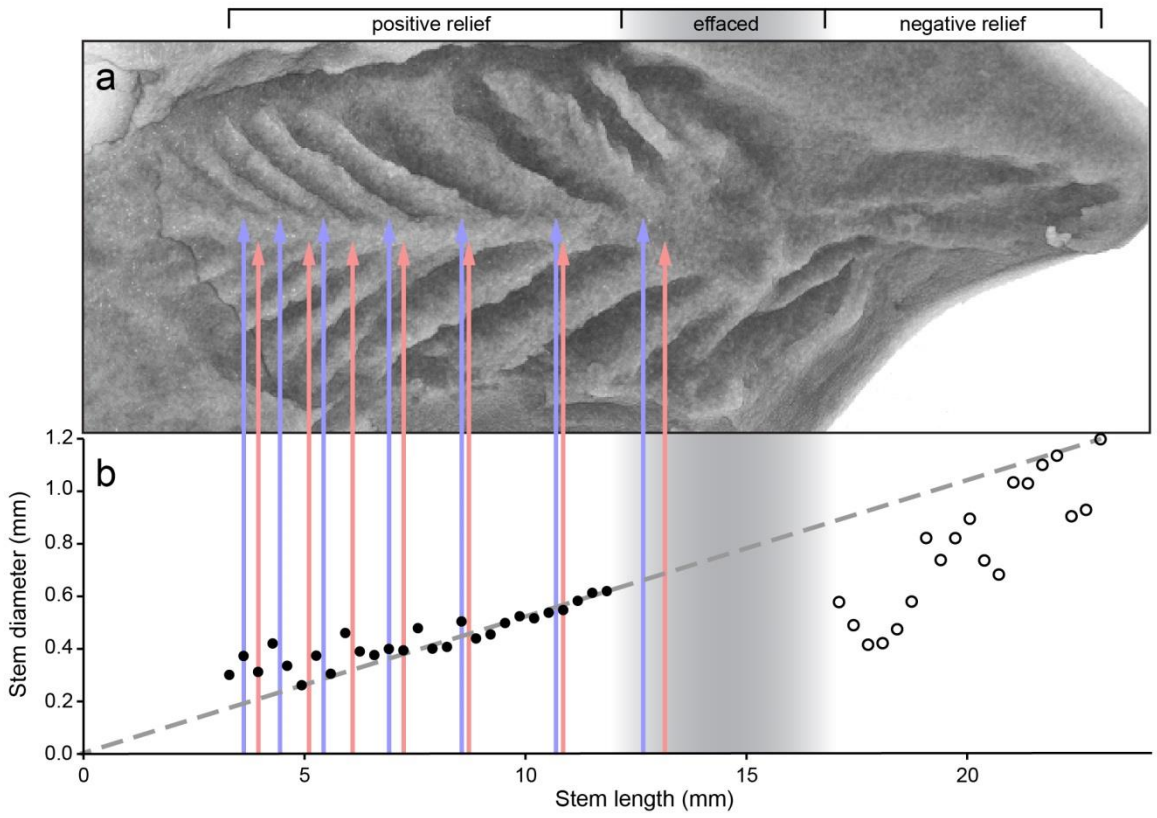

Figure 2

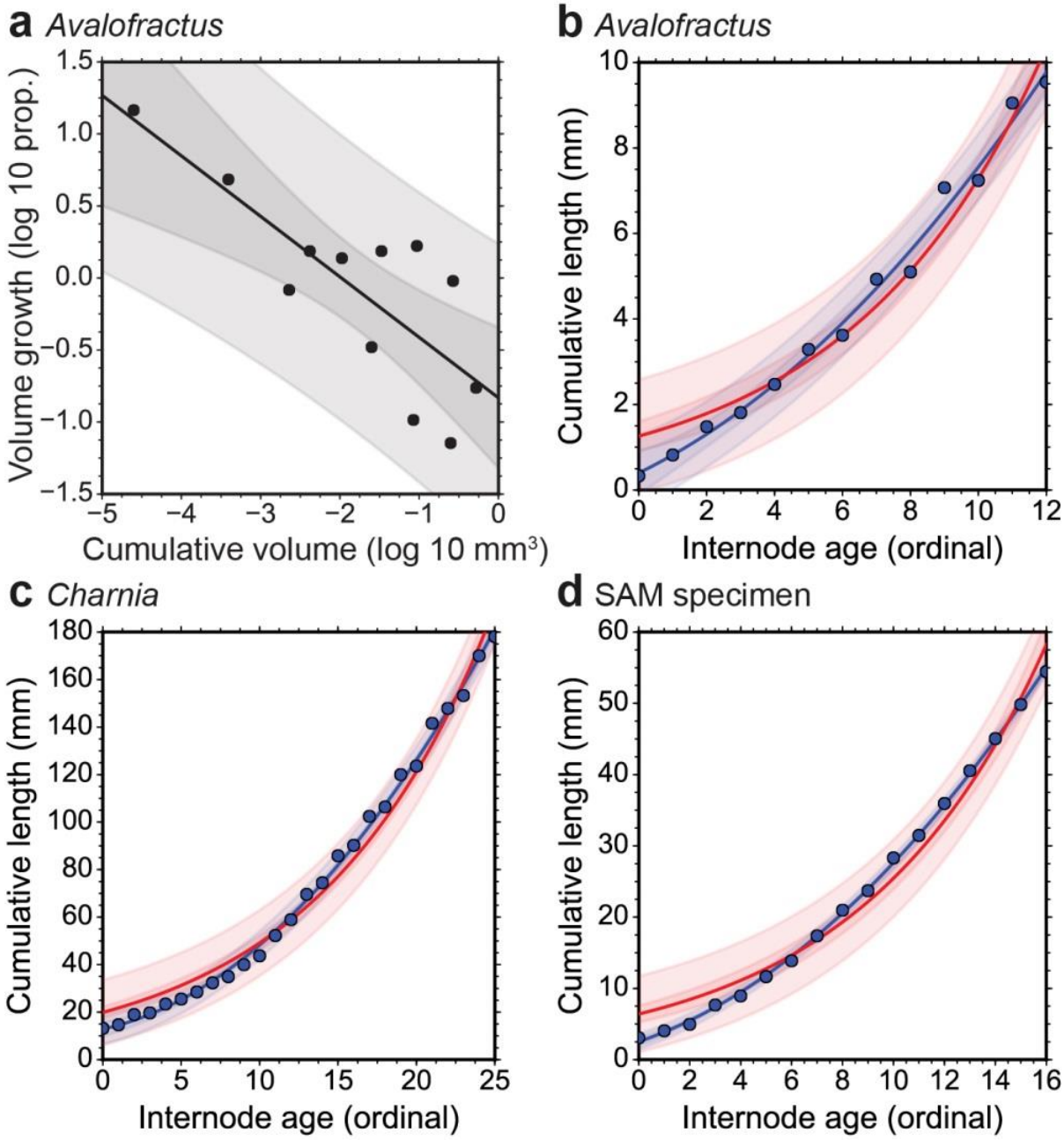
a Avalofractus
Volume growth (log 10 prop.)
Cumulative volume (log 10 mm³)
b Avalofractus
Cumulative length (mm)
Internode age (ordinal)
c Charnia
Cumulative length (mm)
Internode age (ordinal)
d SAM specimen
Cumulative length (mm)
Internode age (ordinal)

Figure 3

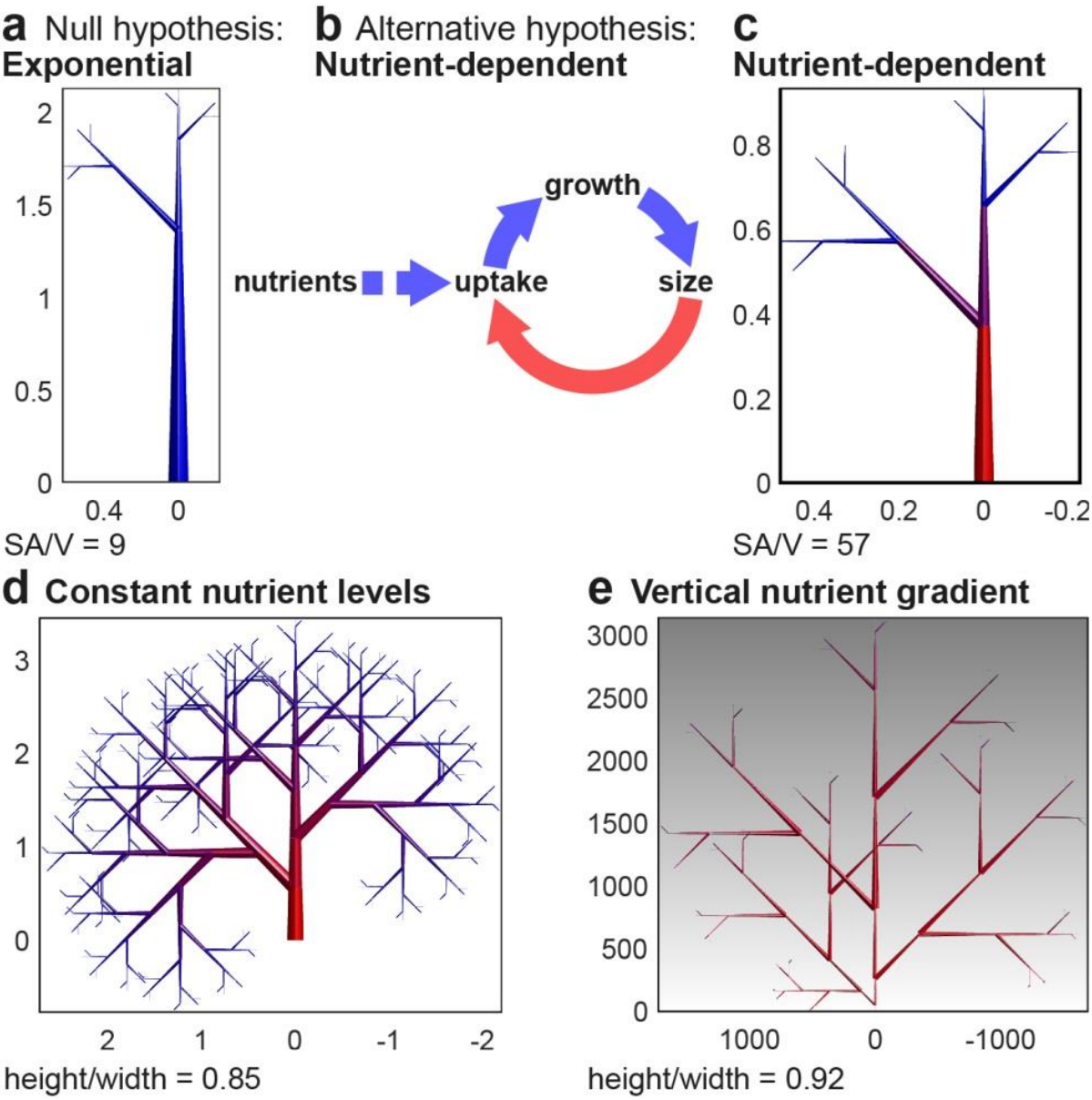
a Null hypothesis:
Exponential
b Alternative hypothesis:
Nutrient-dependent
c
Nutrient-dependent
growth
nutrients
uptake
size
SA/V = 9
SA/V = 57
d Constant nutrient levels
e Vertical nutrient gradient
height/width = 0.85
height/width = 0.92